LAWRENCE
LIVERMORE
NATIONAL
LABORATORY

LLNL-TR-666018

Distinguishing Pu Metal from Pu Oxide and Determining alpha-ratio using Fast Neutron Counting

J. M. Verbeke, G. F. Chapline, L. F. Nakae, M. K. Prasad, S. A. Sheets, N. J. Snyderman

January 9, 2015

Disclaimer

This work performed under the auspices of the U.S. Department of Energy by Lawrence Livermore National Laboratory under Contract DE-AC52-07NA27344.

Distinguishing Pu Metal from Pu Oxide and Determining α-ratio using Fast Neutron Counting

Jérôme M. Verbeke*, George F. Chapline, Leslie F. Nakae,
M. K. Prasad, Steven A. Sheets, N. J. Snyderman
Lawrence Livermore National Laboratory
P.O. Box 808, Livermore, California 94551

Abstract - *We describe a new method for determining the ratio of the rate of (α, n) source neutrons to the rate of spontaneous fission neutrons, the so called α-ratio. This method is made possible by fast neutron counting with liquid scintillator detectors, which can determine the shape of the fast neutron spectrum. The method utilizes the spectral difference between fission spectrum neutrons from Pu metal and the spectrum of (α, n) neutrons from PuO_2. Our method is a generalization of the Cifarelli-Hage method for determining k_{eff} for fissile assemblies, and also simultaneously determines k_{eff} along with the α-ratio.*

I INTRODUCTION

Methods based on time-correlated neutron signals have long been used to characterize fissile materials. Typically one uses ^{3}He tubes to record the arrival times of neutrons from the fissile source, and then by segmenting the arrival times using time windows of varying width, one can use the statistics of the number of neutron counts in the time window as a function of the width of the time window to characterize the neutron source. Unfortunately the cross-section for neutron capture in ^{3}He is only large enough for the purposes of collecting these counting statistics after the fission neutrons have been thermalized in a moderating material. Therefore the time windows must be at least tens of microseconds long to pick up counts from the same spontaneous fission or chain. In the case of a strong neutron source such as Pu this means that many fission chains will be generated within the time windows. Because the neutron time correlations of interest are generated by individual fission chains, the time correlation information that can be extracted using ^{3}He tubes is diluted, requiring high statistics to disentangle the contribution from separate chains.

Liquid scintillators on the other hand, can directly detect unmoderated fission neutrons, because the reaction used for detection is elastic scattering of neutrons primarily on hydrogen, producing a recoil proton from which scintillation light is produced promptly. Consequently, counting can now be on the nanosecond time scale. One no longer needs to open time windows 100's of microseconds long to pick up the correlation signal as with ^{3}He, but only of order 100 nanoseconds. These shorter time windows will enormously reduce the number of overlapping chains within a time window, and we will be in a regime where time windows encompass neutrons from a single fission chain.

In contrast to bare ^{3}He tubes, which can detect only thermal neutrons, liquid scintillators can detect only neutrons above a threshold of about 1 MeV. The threshold is because below an MeV the recoil protons do not produce a sufficiently unique scintillation light pulse to confidently distinguish them from the light pulse

*E-mail: verbeke2@llnl.gov

produced by gamma-ray Compton interactions. The total light collected by the fast proton recoil in the scintillator is statistically proportional to the incident neutron energy. This enables a statistical energy spectrum to be determined. This capability allows the current new analysis.

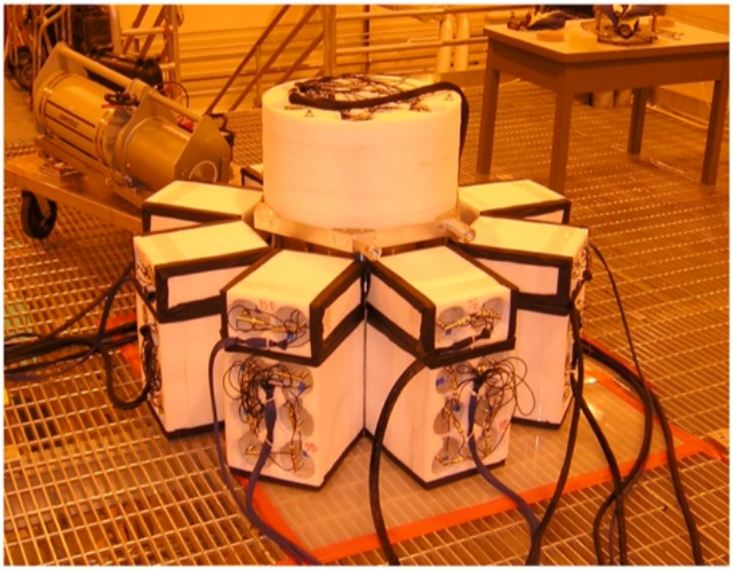

Figure 1: Liquid scintillator array used for measuring the double and triple neutron correlations.

This report describes our efforts to use the time correlations of fast neutrons together with their energy spectra as measured directly in a liquid scintillator array to distinguish Pu metal from Pu oxide and also determine the α-ratio of the Pu oxide[a]. Some earlier work[1,2] had conceptually shown by way of Monte Carlo simulation that this method could work. In this paper, we demonstrate that the method actually works experimentally. The liquid scintillator array used to obtain the results that we will discuss below is illustrated in Fig. 1. If the object at the center of the array contains a multiplying material, each spontaneous fission will typically generate a chain of detected neutrons in the liquid scintillator array. An important difference between Pu metal and Pu oxide is that the α particles produced by the α-decay chain of Pu carry enough energy to cause ^{18}O to emit a neutron via an (α,n) reaction. Although the average energy of this (α,n) reaction is 1.9 MeV, close to the average for fast fission, the energy distributions are different. We will show in the following that these differences can be exploited to determine the α-ratio. These neutrons are emitted randomly, and in the case of Pu oxide the emission rate of these neutrons is comparable to the rate of neutron emission due to spontaneous fission. It is important to note that while the proposed method has been tested successfully for unmoderated systems, its possible application to moderated systems remains yet to be determined.

The key idea is that the count rate, for fast neutron counting, can be partitioned into a contribution with (α,n) spectrum and a contribution with fission spectrum. The separate contributions can be determined from liquid scintillator data by a principal component analysis. The ratio of these contributions gives a relation between α-ratio and multiplication. This enables the Cifarelli-Hage[3,4] correlated moment analysis for determining multiplication given α-ratio to be solved for both quantities.

[a] the α-ratio is the ratio of the (α,n) neutron source strength to the spontaneous fission source strength in units of neutrons/second.

II DESCRIPTION OF PU OBJECTS MEASURED FOR THE REFERENCE NEUTRON SPECTRA

The algorithms developed in this paper rely upon the knowledge of two important neutron energy spectra: (a) the energy spectrum of fission neutrons, and (b) the energy spectrum of O(α,n) neutrons. If these two reference neutron energy spectra are sufficiently distinct, an arbitrary measured neutron energy spectrum should be reconstructable by combining the two reference spectra weighed appropriately.

To produce pure neutron spectra for both fission neutrons and O(α,n) neutrons, we need sources that will primarily produce these neutrons of interest.

II.A Metallic plutonium

For objects containing only gram quantities of plutonium, the system does not multiply, and the neutron emission will be dominated by the spontaneous fission of ^{240}Pu. For kilogram quantities of metallic plutonium, the multiplication can be significant, in which case the fission neutron rate is dominated by induced fissions in ^{239}Pu. In general, the fission neutron energy spectrum will be a mix of ^{240}Pu spontaneous fissions and ^{239}Pu induced fissions. Fortunately, the fission neutron energy spectra for both ^{240}Pu and ^{239}Pu are very similar, as shown in Fig. 2. Therefore, the fission spectrum of objects containing plutonium will be insensitive to multipli-

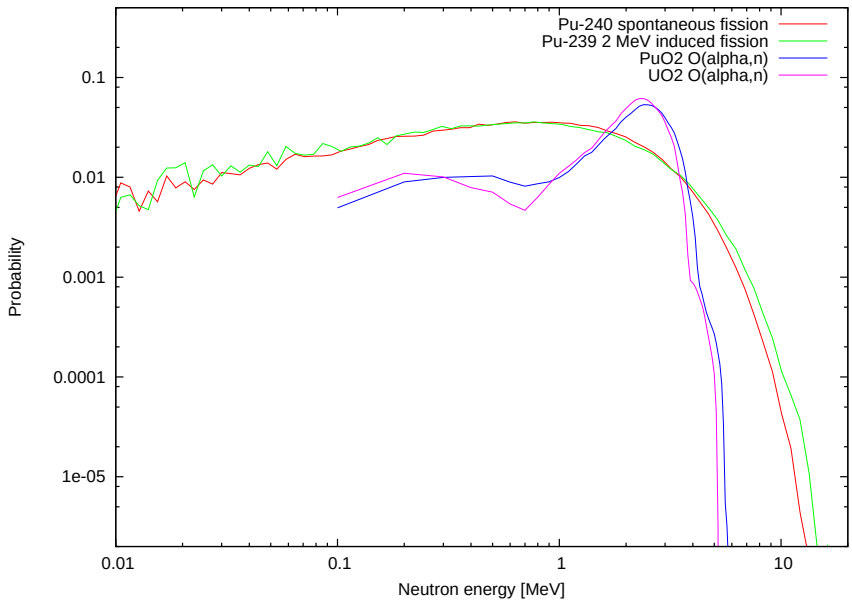

Figure 2: Energy distributions of neutrons from (a) ^{240}Pu spontaneous fission (red), (b) ^{239}Pu 2 MeV induced fission (green), O(α,n) reactions in (c) PuO_2 (blue) and (d) UO_2 (magenta). Fission spectra,[5] (α,n) spectra computed using SOURCE-4C.[6]

cation.

In Fig. 3(b), we show the spectrum of energy deposited in our liquid scintillator by the fission neutrons for a bare 2.35 kg plutonium ball of density 15.92 g/cm^3 consisting of 93.88% ^{239}Pu, 5.96% ^{240}Pu, 0.13% ^{241}Pu,

0.37% ^{241}Am plus trace amounts of other isotopes.

II.B Plutonium dioxide

For the oxide form of plutonium, namely PuO_2, the fast neutron spectrum will also contain a contribution from (α,n) neutrons. We have found from computer simulations that the ratio of the (α,n) neutron rate to the spontaneous fission neutron rate, also referred to as the α-ratio is of the order of 0.8. This α-ratio is a consequence of the fact that ^{240}Pu is a very strong spontaneous fission neutron source, and therefore in general the neutrons coming out of PuO_2 will contain comparable numbers of fission and α,n) neutrons. If we were able to turn off fission reactions for both ^{239}Pu and ^{240}Pu, we could measure the O(α,n) neutron energy spectrum produced by the plutonium decay α-particles. While this would be possible in simulation, fission reactions cannot be turned off in nature. Of course, one might try using a theoretically derived (α,n) neutron spectrum to separate an observed fast neutron spectrum into a fission piece and an (α,n) piece. Unfortunately, converting a theoretical neutron spectrum into a liquid scintillator spectrum would require knowing how to convert an intrinsic neutron energy spectrum into a spectrum of liquid scintillator pulses with the pulse shape that one somewhat arbitrarily identifies as a neutron. This is very difficult to do in practice.

While we have a α-ratio of the order of 0.8 for PuO_2, the α-ratio is of the order of 30 or more for UO_2 (for an uranium composition close to HEU). This means that the vast majority of the neutrons emitted by uranium dioxide are O(α,n) neutrons. Measuring the spectrum of neutrons coming off of UO_2 would be roughly equivalent to measuring the O(α,n) neutrons directly, without much pollution from fission neutrons. If it happened that the energy spectra of the O(α,n) neutrons from PuO_2 and UO_2 are similar, we could substitute PuO_2 with UO_2 to estimate the energy spectrum of PuO_2. Fig. 2 shows the energy distribution of O(α,n) neutrons (mainly from ^{18}O) for both PuO_2 (blue) and UO_2 (magenta). The (α,n) neutron spectra from PuO_2 and UO_2 are very close; therefore when analyzing the fast neutron spectrum from objects containing PuO_2 one can use the UO_2 (α,n) spectrum as a surrogate for the PuO_2 (α,n) spectrum. The objects used for measurement of the O(α,n) spectrum were 3 UO_2 objects of weights 1485.9, 1463.5, and 1516.7 g. The uranium in these objects consisted of 93.4% ^{235}U, 5.7% ^{238}U, 0.86% ^{234}U. The oxygen consisted in 99.8% ^{16}O, 0.04% ^{17}O and 0.2% ^{18}O. The total ^{18}O mass was 1 g, which is the source of the (α,n) neutrons.

The 3 uranium oxide objects were located in the middle of our array of liquid scintillators depicted in Fig. 1. The spectrum of energy deposited in the liquid scintillator by the UO_2 neutrons is shown in blue in Fig. 3(a). Because the UO_2 objects are weak neutron sources, we need to subtract the background that was present during the measurement to get to the UO_2 neutron spectrum. A 15-hour background spectrum was taken within 2 days of the experiment. The neutron energy spectrum from that background measurement is shown in green in Fig. 3(a). The rate of that background is 1.6 n/s and is likely due to cosmic-rays. Since the count rate for the measured objects is 13.52 n/s, the detection system system is measuring background neutrons 12% of the time. Thus, the blue curve in Fig. 3(a) contains both the UO_2 neutrons and 12% of background neutrons. Subtracting the background spectrum in green from the UO_2 spectrum in blue, we obtain the background-suppressed UO_2 neutron spectrum shown in blue in Fig. 3(b).

Regarding the fission neutrons emitted by both the spontaneous fissions of ^{238}U and the induced fissions in ^{235}U, since only 2 to 3% percents of the neutrons are due to fission in UO_2, the red curve in Fig. 3(b) would have to be shifted down by almost 2 orders of magnitude before being subtracted from the blue curve to produce a pure (α,n) neutron spectrum from uranium decay α-particles on oxygen. We can thus see that the normalized U fission curve would very small compared to the observed UO_2 curve, and therefore the effect of subtracting the U fission spectrum would be negligible. Given the resemblance between the (α,n) neutron energy spectra from UO_2 and PuO_2 (see Fig. 2), we will from this point on use the (α,n) neutron energy spectrum from UO_2 as a substitute for the (α,n) neutron energy spectrum for PuO_2.

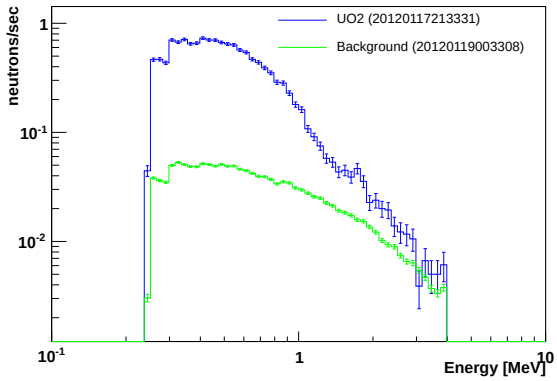

(a) Fast neutron rates versus energy for UO_2 objects (blue) and background (green).

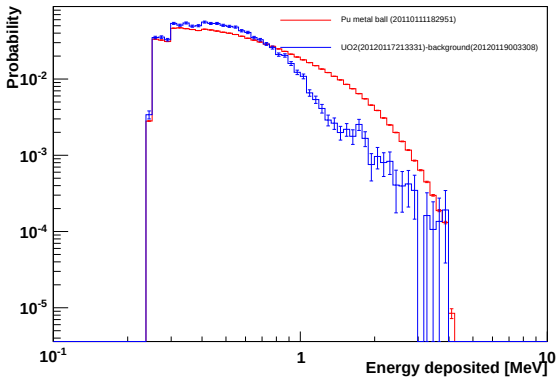

(b) Fast neutron energy spectra for bare Pu metal ball (red) and UO_2 objects where the background was suppressed (blue).

Figure 3: Fast neutron energy spectra. The UO_2 curve represents 1800 s of data, the background 53,442 s, and the Pu metal ball 596 s. The measured count rates for the UO_2 objects, background and Pu metal were 13.52 n/s, 1.6 n/s, and 9123 n/s, respectively.

III MOMENT EQUATIONS WITH DIFFERENT NUCLEAR DATA AND EFFICIENCIES FOR (α,n) NEUTRONS AND FISSION NEUTRONS

The times of arrival of the neutrons in each of the liquid scintillator cells were recorded. Randomly splitting the sequence of time tags into N segments of length T — where T is of the order of nanoseconds to hundreds of microseconds — one can count how many neutrons arrive in the first segment, how many in the second segment, in the third one, etc. and build distributions $b_n(T)$ of the number n of neutrons arriving in the segments of length T. For the sake of illustration, one such count distribution is shown in Fig. 5. By repeating this procedure for segments of different lengths T, multiple count distributions $b_n(T)$ can be obtained.

These count distributions $b_n(T)$ can be used to determine the strength F_s of the spontaneous fission sources in the object, the efficiency ε of the liquid scintillator array, and multiplication M of fissile material.[7] We will show these count distributions can also be used to determine the rate of neutrons from the (α,n) reactions. This will be shown by way of the first three moment equations for the count distributions.

The count rate can be partitioned into a contribution with (α, n) spectrum and a contribution with fission spectrum,

$$R_1 = S_\alpha q_\alpha \varepsilon_\alpha + F_s \bar{\nu}_s \varepsilon q M + S_\alpha p_\alpha \bar{\nu}_\alpha \varepsilon q M. \tag{1}$$

The three contributions to Eq. (1) are illustrated in Figs. 4. The first term is due to (α, n) neutrons that escape without inducing fission, Fig. 4(c). Because of the spectrum difference of efficiency for the liquid scintillator detectors, ε_α can be different from ε. The second term is the usual count rate from spontaneous fission induced chains, Fig. 4(a). The last term is due to (α,n) neutron induced fission. As noted by Böhnel[8] and Hage-Cifarelli,[4] the probability for an (α, n) neutron to induce fission is in general different from a fission spectrum neutron. (This is most obvious for ^{9}Be(α,n)^{12}C, where the high energy neutron induces fission with a higher probability p_α than fission spectrum, and with a higher $\bar{\nu}_\alpha$.) Also $q_\alpha = 1 - p_\alpha$, the probability for neutron escape can be different for (α,n) spectrum neutrons that fission spectrum. It is further assumed that the induced fission by the (α,n) neutron emits neutrons with a fission spectrum. The (α,n) neutron induced fission acts like an effective spontaneous fission for the rest of the chain, Fig. 4(b).

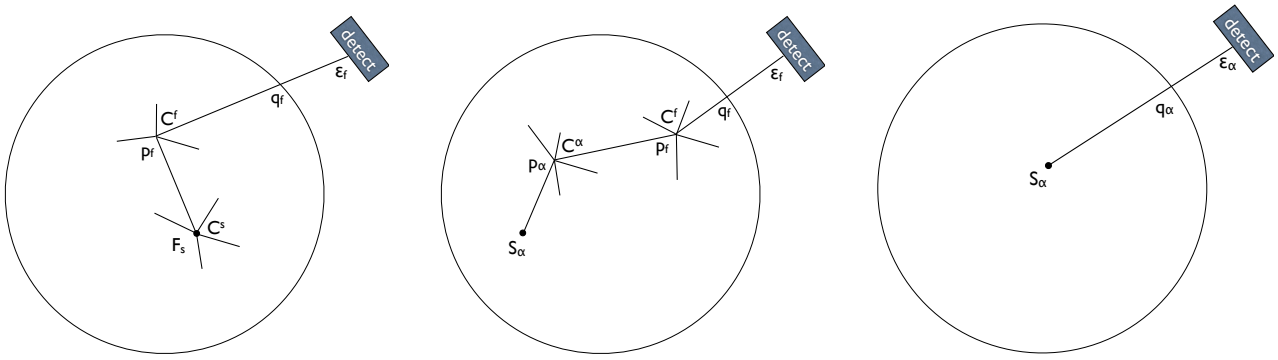

(a) Fission chains generated by spontaneous fission neutrons.

(b) Fission chains generated by (α,n) neutrons.

(c) Direct (α,n) neutron detection.

Figure 4: Three classes of neutrons contributing to the detector.

The ratio of neutron source rates is the α-ratio, here denoted A, [b]

$$A = \frac{S_\alpha}{\bar{\nu}_s F_s}.$$

For time-gated fast neutron counting, the time dependent second and third moments of the random time gate distribution $b_n(T)$ are a generalization of the formulas given by Prasad-Snyderman.[7] Normalizing by the count rate,

$$Y_{2F}(T) = \frac{(\varepsilon q M)^2}{(\varepsilon q M)(1+p_\alpha \bar{\nu}_\alpha A)+\varepsilon_\alpha q_\alpha A}\left[D_{2s}+\bar{\nu}_\alpha p_\alpha A D_{2\alpha}+D_2(M-1)(1+\bar{\nu}_\alpha p_\alpha A)\right]\left(1-\frac{1-e^{-\alpha T}}{\alpha T}\right) \tag{2}$$

$$\begin{aligned} Y_{3F}(T) = &\frac{(\varepsilon q M)^3}{(\varepsilon q M)(1+p_\alpha \bar{\nu}_\alpha A)+\varepsilon_\alpha q_\alpha A}\left[D_{3s}+p_\alpha \bar{\nu}_\alpha A D_{3\alpha}+(M-1)(1+p_\alpha \bar{\nu}_\alpha A)D_3\right]\left(1-\frac{3-4e^{-\alpha T}+e^{-2\alpha T}}{2\alpha T}\right) \\ &+\frac{(\varepsilon q M)^3}{(\varepsilon q M)(1+p_\alpha \bar{\nu}_\alpha A)+\varepsilon_\alpha q_\alpha A}\left[2D_2(M-1)(D_{2s}+p_\alpha \bar{\nu}_\alpha A D_{2\alpha})+2(M-1)^2 D_2^2(1+p_\alpha \bar{\nu}_\alpha A)\right]\left(1-\frac{2-(2+\alpha T)e^{-\alpha T}}{\alpha T}\right) \end{aligned} \tag{3}$$

For the correlated triples, the two terms with different time dependences correspond to the following topological classes [c]: in the first term, all counted neutrons have a single common ancestor, while for the second time dependence term two of the counted neutrons have a common ancestor fission, and the third counted neutron has an ancestor with the neutron that induced that fission.

[b] For ^{3}He counting the efficiencies are the same. Further, for PuO_2, q_α can be approximated by q. With these simplifications,

$$\begin{aligned} R_1 &= \varepsilon q S_\alpha + \varepsilon q M \bar{\nu}_s F_s + \varepsilon q M S_\alpha p \bar{\nu} \\ &= \varepsilon q M \bar{\nu}_s F_s + \varepsilon q S_\alpha [1+\bar{\nu} p M]. \end{aligned}$$

Because $pM = \frac{M-1}{\bar{\nu}}$, the term in square brackets becomes $[1+(M-1)] = M$, so

$$R_1 = \varepsilon q M \bar{\nu}_s F_s (1+A).$$

[c] For ^{3}He counting, both topological classes have the same time dependence, comparable to that of the first term of Eq. (3).

In contract with ^{3}He counting, the ratio of the two terms in Eq. (1) becomes measurable for fast counting,

$$\begin{aligned}\rho &= \frac{S_\alpha q_\alpha \varepsilon_\alpha}{(\varepsilon q M)\left[F_s \bar{\nu}_s + S_\alpha p_\alpha \bar{\nu}_\alpha\right]} \\ &= \frac{A q_\alpha \varepsilon_\alpha}{(\varepsilon q M)\left[1 + A p_\alpha \bar{\nu}_\alpha\right]}.\end{aligned}$$

The approximations for PuO_2 are that (a) $p_\alpha \simeq p$, so $q_\alpha \simeq q$ and (b) $\bar{\nu}_\alpha \simeq \bar{\nu}$, so that

$$\begin{aligned}\rho &= \frac{A\frac{\varepsilon_\alpha}{\varepsilon}\frac{q_\alpha}{q}}{M + A p_\alpha \bar{\nu}_\alpha M} \\ &\simeq \frac{A\frac{\varepsilon_\alpha}{\varepsilon}}{1 + (M-1) + A(M-1)} \\ &= \frac{A r_\varepsilon}{1 + (M-1)(1+A)}.\end{aligned} \tag{4}$$

The ratio $r_\varepsilon = \frac{\varepsilon_\alpha}{\varepsilon}$ is an intrinsic property of the liquid scintillator spectral response, and can be determined. For our liquid scintillators we find $r_\varepsilon \simeq 1.6$. For PuO_2, the additional measured quantity defined in Eq. (4) will turn out to give an additional relation between M and A, and enable one to determine both A and M by the Cifarelli-Hage moment method.

With the relation provided in Eq. (4), the Cifarelli-Hage equation becomes

$$\frac{R_{2F}^2}{R_{3F}} = \frac{\left[D_{2s} + (1+A)(M-1)D_2\right]^2}{D_{3s}(1+A) + 2(1+A)(M-1)D_{2s}D_2 + 2\left[(M-1)(1+A)\right]^2 D_2^2 + (1+A)(M-1)D_3(1+A)} \tag{5}$$

For A=0, this formula is the familiar Hage-Cifarelli equation for M. For A$\neq$0, all the M dependence is in the combination $(1+A)(M-1)$, and this can be expressed in terms of the measured ρ, and the unknown A using Eq. (4),

$$(1+A)(M-1) = \frac{r_\varepsilon A}{\rho} - 1. \tag{6}$$

Substituting Eq. (6) into Eq. (5), we find that A satisfies the following quadratic equation:

$$2D_2\left(\frac{r_\varepsilon}{\rho}A - 1\right)\left[D_{2s} + D_2\left(\frac{r_\varepsilon}{\rho}A - 1\right)\right] + (A+1)\left(D_{3s} + \left(\frac{r_\varepsilon}{\rho}A - 1\right)D_3\right) = \frac{\frac{\rho}{r_\varepsilon}+1}{\rho+1}\left[D_{2s} + \left(\frac{r_\varepsilon}{\rho}A - 1\right)D_2\right]^2 \frac{R_{3F}}{R_{2F}^2} \tag{7}$$

After solving Eq. (7) for A, Eq. (6) then determines M. In the next sections, we show that this equation, together with the neutron spectral information provided by the liquid scintillators, can be used to measure both the α-ratio and the multiplication of plutonium oxide samples of interest.

IV LIQUID SCINTILLATOR TIME CORRELATION RESULTS

For the 2.35 kg Pu ball previously described, the count distribution for T=1 μs, and the moments $Y_{2F}(T)$ and $Y_{3F}(T)$ are shown in Fig. 5. The total time is shared among the 6 time gates in such a way as to keep the errors on the $Y_{2F}(T)$ and $Y_{3F}(T)$ values for the different time gates approximately equal. Fast neutron counts are not re-used among different time gates. These data correspond to a measurement of 113 seconds, 21.2 seconds of which contributed to the 1 μs time gate, and the remaining time was shared among the other time gates. The values of R_1, R_{2F} and R_{3F} can be extracted from the graphs by fitting the data to the time dependence, $\bar{C} = R_1 T$, and for $Y_{2F}(T)$, Eq. (2), and for $Y_{3F}(T)$, Eq. (3).

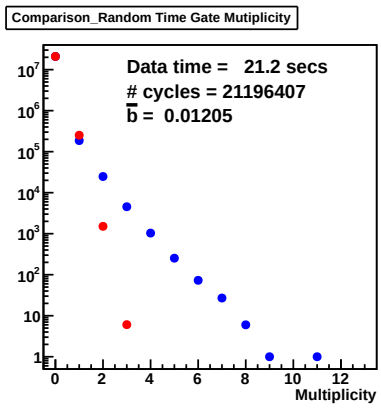

(a) Count distribution $b_n\,(T = 1\ \mu s)$.

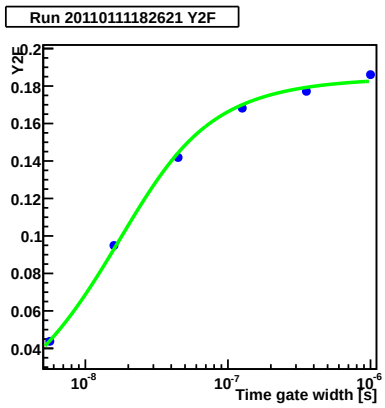

(b) $Y_{2F}\,(T)$. Measured (blue) versus theoretical reconstruction (green, Eq. (2)).

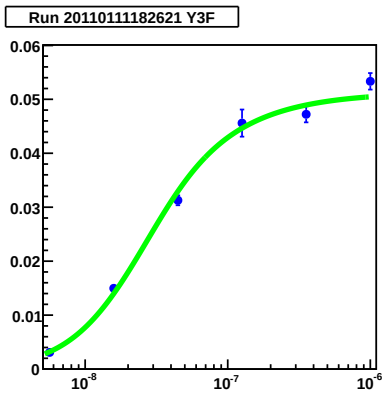

(c) $Y_{3F}\,(T)$. Measured (blue) versus theoretical reconstruction (green, Eq. (3)).

Figure 5: Count distribution and moments for Pu metal ball. T between 5 ns and 1 μs. The set of parameters used for the moment reconstruction (M,ε,α)=(2.1, 4.6%, 0.006) was determined using the measured moments and spectral information.

Fig. 6 shows the results for a PuO_2 sample containing 8.72 g of plutonium. The measurement thereof was much longer as the weight of PuO_2 was just a few grams.

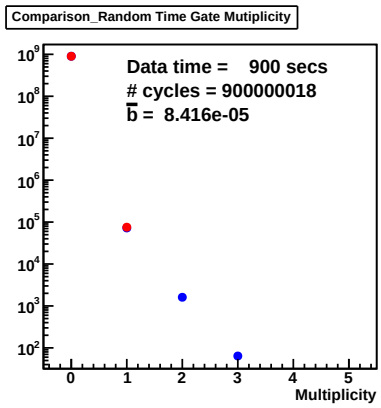

(a) Count distribution $b_n\,(T = 1\ \mu s)$.

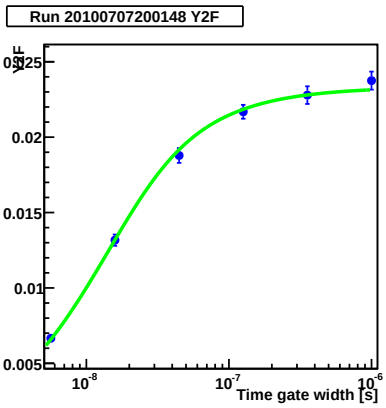

(b) $Y_{2F}\,(T)$. Measured (blue) versus theoretical reconstruction (green, Eq. (2)).

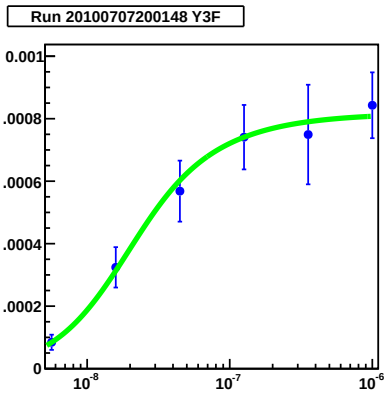

(c) $Y_{3F}\,(T)$. Measured (blue) versus theoretical reconstruction (green, Eq. (3)).

Figure 6: Count distribution and moments for PuO_2 sample. T between 5 ns and 1 μs. The set of parameters used for the moment reconstruction (M,ε,α)=(1.06, 5.1%, 0.86) was determined using the measured moments and spectral information.

V LIQUID SCINTILLATORS SPECTRAL INFORMATION

In this section we describe experimental results which illustrate how the information contained in the spectrum of energies deposited by the fast neutrons in the liquid scintillator cells can be used to differentiate metallic

plutonium from plutonium dioxide. For the measured PuO_2 sample, the spectrum of energies deposited by the fast neutrons is shown in green in Fig 7, along with the Pu metal neutron spectrum in red and the pure (α,n) neutron spectrum from α-particles on oxygen in blue (the latter two directly copied from Fig. 3(b)). In Fig. 8

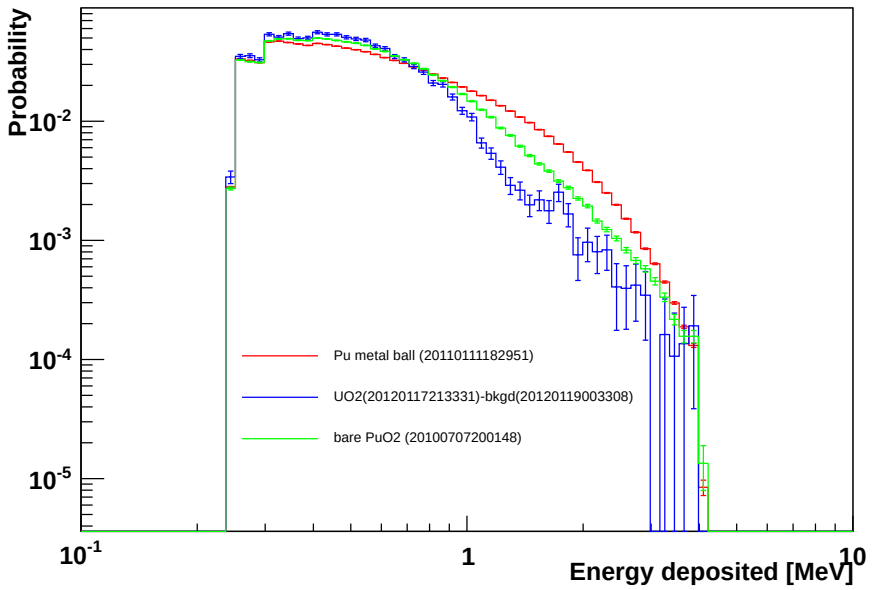

Figure 7: Fast neutron energy spectra for PuO_2 sample (green), along with Pu metal ball (red) and modified UO_2 (blue) spectra. The experimental curve for PuO_2 represents 7200 s of data.

we show that the red and blue spectra can be added with suitable weights to reconstruct the green curve. In particular, by adding the ^{240}Pu spectrum pre-multiplied by 0.45 to the (α,n) spectrum pre-multiplied by 0.55, one obtains the reconstruction spectrum of energies deposited shown in red in Fig. 8(b). On the other hand, when one measures the Pu metal ball, the weights that are optimal for the reconstruction of the spectrum of deposited energies are 0.995 of the ^{240}Pu spectrum and 0.005 of the (α,n) spectrum. So we find that just measuring the spectrum of energies deposited in a liquid scintillator by fast neutrons is sufficient to distinguish Pu metal and Pu oxide.

Setting ρ=1.24, the solution to Eqs. (6) and (7) with $M \geq 1$ is $A = 0.86 \pm 0.08$, $M = 1.06 \pm 0.09$. The exact value of 0.8 for A is within 1 standard deviation of our solution. Using $R_{2F} = R_2/R_1$ calculated from Eqs. (1) and (A.14), we determined the value of ε to be 5.1%, while Eq. (1) implies a spontaneous fission source rate of 662 ± 57 neutrons/sec. Although not exactly the same strength as the true value of 519 n/s, the implied spontaneous fission rate is within 20% of the correct answer. If we measure 10 times longer, the solution with $M \geq 1$ becomes $A = 0.84 \pm 0.02$, $M = 1.05 \pm 0.02$, ε=5.3%, and the spontaneous fission source rate becomes 638 ± 11 neutrons/sec. For the metallic plutonium ball, our algorithm gives ρ=0.005. The solution to Eqs. (6)-(7) with $M \geq 1$ is $A = 0.006 \pm 0.0001$, $M = 2.1 \pm 0.04$. The value of ε is 4.6% and the source strength is $149,015 \pm 2,700$ neutrons/sec, which is off the true value by less than 1.5%, or less than 1 standard deviation.

VI CONCLUSION

In this paper, we have shown first of all that measuring the energy spectrum of the fast neutrons using a liquid scintillator allows one to immediately distinguish the metallic and oxide forms of plutonium. In addition, com-

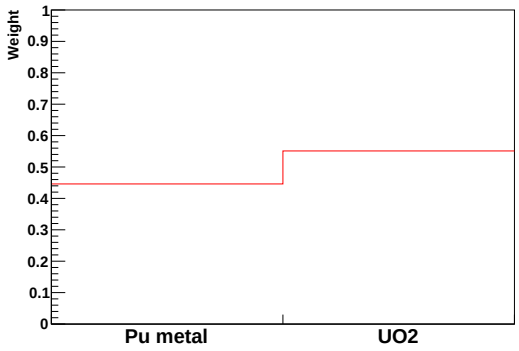

(a) Factors by which the blue and red spectra shown in Fig. 7 must be multiplied to reconstruct the spectrum of energies deposited by the fast neutrons emitted by the PuO_2 sample: 0.45 for the Pu metal spectrum and 0.55 for the UO_2 sample spectrum.

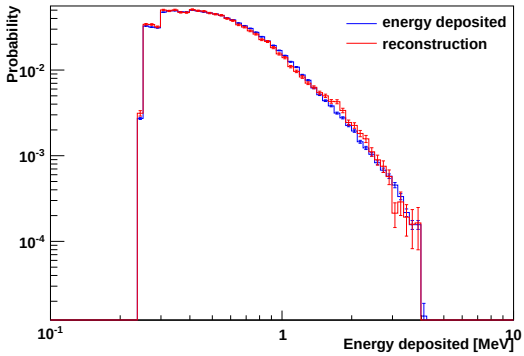

(b) Spectrum of energies deposited by fast neutrons in liquid scintillator cells for the PuO_2 sample (blue), along with its reconstruction (red) from the blue and red spectra shown in Fig. 7 and the optimal weights shown on the left.

Figure 8: Reconstruction of the PuO_2 objects using the sum of two weighed energy spectra.

bining this spectral information with the Feynman 2-neutron and 3-neutron correlations allows one to extract the α-ratio without explicitly knowing the multiplication. Given the α-ratio one can then extract the multiplication as well as the ^{239}Pu and ^{240}Pu masses directly from the moment equations. In principle the same techniques could be used to distinguish metallic Pu from other compounds of Pu, such as PuF_2, where (α,n) neutron emission is also significant.

ACKNOWLEDGMENTS

This work was performed under the auspices of the U.S. Department of Energy by Lawrence Livermore National Laboratory under Contract DE-AC52-07NA27344. The authors wish to acknowledge the Office of Defense Nuclear Nonproliferation Research and Development in DOE/NNSA for their support.

A DERIVATION USING GENERATING FUNCTION

Eq. A.16 of Prasad *et al.*[9] gives the random time gate count distribution generating function for fission chains initiated by single neutrons. The formulas of Prasad *et al.*[9] are appropriate for ^{3}He counting, but the asymptotic limit $T \to \infty$ gives the same expressions as for fast counting.[10] We use this to derive the expressions for R_i below. In the limit of $\lambda T \gg 1$, the two exponential terms[d] $e^{-\lambda t}$ become negligible and we get

$$\lim_{\lambda T \gg 1} \ln\left(\Pi\left(y,T\right)\right) \to ST\left[h\left(1-\varepsilon\left(1-y\right)\right)-1\right] \tag{A.1}$$

where S is the neutron source strength, T is the time gate width, h is the Böhnel[8] fission chain generating function, y is the generating function variable, and ε is the fission neutron detection efficiency.

[d] typographical error in Eq. A.16 of Prasad *et al.*:[9] the two exponentials $e^{-\lambda T}$ in the integrand should read $e^{-\lambda t}$.

Spontaneous fission initiated chain. Fig. 4(a) shows a fission chain initiated by a spontaneous fission. The rate of spontaneous fissions is F_s in units of spontaneous fissions per second. Spontaneous fissions will produce a number of neutrons sampled from a distribution C_n^s. Each one of these fission neutrons has a probability p of inducing a subsequent fission, which will in turn produce a number of neutrons sampled from a distribution C_n. Neutrons of the fission chain initiated by spontaneous fission can leak with probability q, and have a probability ε of being recorded. For fission chains initiated by spontaneous fissions, Eq. C.7 of Prasad *et al.*[9] indicates that $\ln(\Pi(y,T))$ should be[e]

$$\lim_{\lambda T \gg 1} \ln(\Pi(y,T)) \to F_s T\left(C^s\left[h\left(1-\varepsilon\left(1-y\right)\right)\right]-1\right) \tag{A.2}$$

Fig. 4(b) and 4(c) show the contributions from (α,n) neutrons.

Direct (α,n) neutron detector count. The neutrons created by the (α,n) reaction will leak with a probability q_α ($q_\alpha = 1-p_\alpha$), before they induce any fissions, and will be detected with probability ε_α, as shown in Fig. 4(c). Therefore, we need a term:

$$+S_\alpha T q_\alpha\left[1-\varepsilon_\alpha\left(1-y\right)\right] \tag{A.3}$$

where ε_α is the (α,n) neutron detection efficiency.

Induced fission contribution. Spontaneous fissions are not the only source of fission chains. Each (α,n) neutron has a probability p_α of inducing a fission, which produces a number of neutrons sampled from a distribution C_n^α. For PuO_2 it is a good approximation that following this first induced fission the rest of the fission chain turns into a fission chain of the type shown in Fig. 4(a), with properties p and C_n. The term

$$+S_\alpha T p_\alpha C^\alpha\left[h\left(1-\varepsilon\left(1-y\right)\right)\right] \tag{A.4}$$

is added to $\ln(\Pi(y,T))$ to account for the (α,n) neutron initiated fission chains. $S_\alpha = A\bar{\nu}_s F_s$ is the (α,n) neutron source strength in units of neutrons per second.

The complete equation[f] for $\ln(\Pi(y,T))$ thus reads

$$\lim_{\lambda T \gg 1} \ln(\Pi(y,T)) \to F_s T\left(C^s\left[h\left(1-\varepsilon\left[1-y\right]\right)\right]-1\right)+S_\alpha T\left(p_\alpha C^\alpha\left[h\left(1-\varepsilon\left(1-y\right)\right)\right]+q_\alpha\left[1-\varepsilon_\alpha\left(1-y\right)\right]-1\right) \tag{A.5}$$

For y=1, this expression vanishes, corresponding to $\Pi(y,T) = \sum_{n=0}^{\infty} b_n(T) = 1$. For the chain rule differentiations that follow, it is convenient to define the functions

$$z(y) = 1-\varepsilon\left(1-y\right), \qquad \frac{\partial z}{\partial y} = \varepsilon, \tag{A.6}$$

[e] typographical error in Eq. C.7 of Prasad *et al.*:[9] the left hand side should be $C^s[h(y)]$

[f] This generalization reduces, for the terms in Eq. A.5 proportional to S_α, to Eq. A.1 in the particular case where (α,n) neutrons have the same energy spectrum as fission neutrons, i.e. $p_\alpha = p$, $q_\alpha = q$, $C_n^\alpha = C_n$, and $\varepsilon_\alpha = \varepsilon$. Using Böhnel's equation $h(z) = qz + pC[h(z)]$, the term factor of $S_\alpha T$ in Eq. A.7 reduces to Eq. A.1:

$$ST\left(pC_n\left[h\left(z\right)\right]+qz-1\right) = ST\left(h\left(z\right)-1\right)$$

and similarly for z_α, to rewrite Eq. A.5 as

$$\ln\left(\Pi\left(y,T\right)\right) \rightarrow F_{\mathrm{s}} T\left(C^{\mathrm{s}}\left[h\left(z\right)\right]-1\right)+S_\alpha T\left(p_\alpha C^\alpha\left[h\left(z\right)\right]+q_\alpha z_\alpha-1\right) \tag{A.7}$$

For the sake of the remaining part of this chapter, it is convenient to rewrite Böhnel[8]'s Eqs. 21-23 using $M=1/(1-p\bar{\nu})$ and $q=1-p$:

$$\begin{aligned}
\left.\frac{\partial h}{\partial y}\right|_{y=1} &= qM \\
\left.\frac{1}{2!}\frac{\partial^2 h}{\partial y^2}\right|_{y=1} &= D_2\left(M-1\right)\left(qM\right)^2 \\
\left.\frac{1}{3!}\frac{\partial^3 h}{\partial y^3}\right|_{y=1} &= \left(qM\right)^3\left[D_3\left(M-1\right)+2\left(M-1\right)^2 D_2^2\right]
\end{aligned} \tag{A.8}$$

where $D_2=\nu_2/\bar{\nu}$, $D_3=\nu_3/\bar{\nu}$. The average number of neutrons emitted in induced fission is

$$\bar{\nu}=\sum_{\nu=1}^{\nu_{\max}} \nu C_\nu, \tag{A.9}$$

In general, the fractional moments of the C_ν distribution, $\nu_n=\sum_{\nu=n}^{\nu_{\max}}\binom{\nu}{n}C_\nu$, can be determined by derivatives of the generating function:

$$\nu_{\mathrm{n}}=\frac{1}{n!}\left.\frac{\partial^n C\left(x\right)}{\partial x^n}\right|_{x=1} \qquad \text{for } n\geq 1. \tag{A.10}$$

Using Eqs. 115 and 118 of Prasad-Snyderman,[7] and also Eq. A.8 of Hage-Cifarelli,[4] it can be shown that

$$\ln\left(\Pi\left(y,T\right)\right)=\sum_{k=1}^{\infty} Y_k\left(T\right)\left(y-1\right)^k. \tag{A.11}$$

This relation is true for fast counting as well. We define the R_i's as

$$R_i T=\lim_{T\rightarrow\infty} Y_i\left(T\right). \tag{A.12}$$

Taking the derivatives of $\ln\left(\Pi\left(y,T\right)\right)$ in Eq. A.7 and using Eq. A.6, we get

$$\begin{aligned}
R_1 =& \frac{1}{T}\left.\frac{\partial \ln\left(\Pi\left(y,T\right)\right)}{\partial y}\right|_{y=1} \\
=& F_{\mathrm{s}}\left.\left(\frac{\partial C^{\mathrm{s}}}{\partial h}\frac{\partial h}{\partial z}\frac{\partial z}{\partial y}\right)\right|_{y=1}+S_\alpha\left.\left(p_\alpha\frac{\partial C^\alpha}{\partial h}\frac{\partial h}{\partial z}\frac{\partial z}{\partial y}+q_\alpha\frac{\partial z_\alpha}{\partial y}\right)\right|_{y=1} \\
=& \varepsilon qM\bar{\nu}_{\mathrm{s}}F_{\mathrm{s}}+\left(\varepsilon qMp_\alpha\bar{\nu}_\alpha+\varepsilon_\alpha q_\alpha\right)S_\alpha
\end{aligned} \tag{A.13}$$

The second derivative reads

$$\begin{aligned}
R_2 =& \frac{1}{2T}\lim_{\lambda T\gg 1}\left.\frac{\partial^2 \ln\left(\Pi\left(y,T\right)\right)}{\partial y^2}\right|_{y=1} \\
=& \frac{1}{2}F_{\mathrm{s}}\varepsilon\left.\left(\frac{\partial^2 C^{\mathrm{s}}}{\partial h^2}\left(\frac{\partial h}{\partial y}\right)^2\frac{\partial z}{\partial y}+\frac{\partial C^{\mathrm{s}}}{\partial h}\frac{\partial^2 h}{\partial y^2}\frac{\partial z}{\partial y}\right)\right|_{y=1}+\frac{1}{2}S_\alpha p_\alpha\varepsilon\left.\left(\frac{\partial^2 C^\alpha}{\partial h^2}\left(\frac{\partial h}{\partial y}\right)^2\frac{\partial z}{\partial y}+\frac{\partial C^\alpha}{\partial h}\frac{\partial^2 h}{\partial y^2}\frac{\partial z}{\partial y}\right)\right|_{y=1} \\
=& \left(\varepsilon qM\right)^2\left[\left[D_{2s}+D_2\left(M-1\right)\right]\bar{\nu}_{\mathrm{s}}F_{\mathrm{s}}+\left[D_{2\alpha}+D_2\left(M-1\right)\right]\bar{\nu}_\alpha p_\alpha S_\alpha\right] \\
=& \left(\varepsilon qM\right)^2\left[D_{2s}+\bar{\nu}_\alpha p_\alpha AD_{2\alpha}+D_2\left(M-1\right)\left(1+\bar{\nu}_\alpha p_\alpha A\right)\right]\bar{\nu}_{\mathrm{s}}F_{\mathrm{s}}
\end{aligned} \tag{A.14}$$

and the third derivative reads

$$
\begin{aligned}
R_3 =& \frac{1}{3!T}\lim_{\lambda T\gg 1}\left.\frac{\partial^3 \ln\left(\Pi\left(y,T\right)\right)}{\partial y^3}\right|_{y=1} \\
=& \frac{1}{3!}F_s\varepsilon^2\left(\frac{\partial^3 C^s}{\partial h^3}\left(\frac{\partial h}{\partial y}\right)^3\frac{\partial z}{\partial y}+2\frac{\partial^2 C^s}{\partial h^2}\frac{\partial h}{\partial y}\frac{\partial^2 h}{\partial y^2}\frac{\partial z}{\partial y}+\frac{\partial^2 C^s}{\partial h^2}\frac{\partial h}{\partial y}\frac{\partial^2 h}{\partial y^2}\frac{\partial z}{\partial y}+\frac{\partial C^s}{\partial h}\frac{\partial^3 h}{\partial y^3}\frac{\partial z}{\partial y}\right)\Bigg|_{y=1} \\
&+\frac{1}{3!}S_\alpha p_\alpha\varepsilon^2\left(\frac{\partial^3 C^\alpha}{\partial h^3}\left(\frac{\partial h}{\partial y}\right)^3\frac{\partial z}{\partial y}+2\frac{\partial^2 C^\alpha}{\partial h^2}\frac{\partial h}{\partial y}\frac{\partial^2 h}{\partial y^2}\frac{\partial z}{\partial y}+\frac{\partial^2 C^\alpha}{\partial h^2}\frac{\partial h}{\partial y}\frac{\partial^2 h}{\partial y^2}\frac{\partial z}{\partial y}+\frac{\partial C^\alpha}{\partial h}\frac{\partial^3 h}{\partial y^3}\frac{\partial z}{\partial y}\right)\Bigg|_{y=1} \\
=& \left(\varepsilon qM\right)^3\Bigg[\left[D_{3s}+2D_{2s}D_2\left(M-1\right)+D_3\left(M-1\right)+2\left(M-1\right)^2D_2^2\right]\bar{v}_s F_s \\
&+\left[D_{3\alpha}+2D_{2\alpha}D_2\left(M-1\right)+D_3\left(M-1\right)+2\left(M-1\right)^2D_2^2\right]\bar{v}_\alpha p_\alpha S_\alpha\Bigg] \\
=& \left(\varepsilon qM\right)^3\left[D_{3s}+p_\alpha\bar{v}_\alpha AD_{3\alpha}+2D_2\left(M-1\right)\left(D_{2s}+p_\alpha\bar{v}_\alpha AD_{2\alpha}\right)+\left(M-1\right)\left(D_3+2\left(M-1\right)D_2^2\right)\left(1+p_\alpha\bar{v}_\alpha A\right)\right]\bar{v}_s F_s
\end{aligned}
\tag{A.15}
$$

For $T\gg\alpha^{-1}$, $Y_{2F}\left(T\right)\rightarrow R_{2F}=R_2/R_1$ of Eqs. A.14 and A.13, and $Y_{3F}\left(T\right)\rightarrow R_{3F}=R_3/R_1$ of Eqs. A.15 and A.13.

References

[1] J.M. VERBEKE, G.F. CHAPLINE, "Distinguishing Plutonium Metal From Plutonium Oxide," LLNL-TR-518451, Lawrence Livermore National Laboratory (2011). 2

[2] J.M. VERBEKE, G.F. CHAPLINE, "Distinguishing Plutonium Metal From Plutonium Oxide Using Fast Neutrons, Preliminary Experimental Results," LLNL-TR-599212, Lawrence Livermore National Laboratory (2012). 2

[3] D.M. CIFARELLI, W. HAGE, "Models for a Three-Parameter Analysis of Neutron Signal Correlation Measurements for Fissile Material Assay," *Nucl. Instr. Meth. Phys. Res.* **A251**, 550-563 (1986). 2

[4] W. HAGE, D.M. CIFARELLI, "Correlation Analysis with Neutron Count Distributions in Randomly or Signal Triggered Time Intervals for Assay of Special Fissile Materials," *Nucl. Sci. Eng.* **89**, 159-176 (1985). 2, 5, 12

[5] J.M. VERBEKE, C. HAGMANN, D. WRIGHT, "Simulation of Neutron and Gamma Ray Emission from Fission and Photofission," LLNL-AR-228518, Lawrence Livermore National Laboratory (2010). 3

[6] W.B. WILSON, R.T. PERRY, E.F. SHORES, W.S. CHARLTON, T.A. PARISH, G.P. ESTES, T.H. BROWN, E.D. ARTHUR, M. BOZOIAN, T.R. ENGLAND, D.G. MADLAND, AND J.E. STEWART, "SOURCES 4C: A Code for Calculating (alpha,n), Spontaneous Fission, and Delayed Neutron Sources and Spectra," LA-UR-02-1839, Los Alamos National Laboratory (2002). 3

[7] M.K. PRASAD, N.J. SNYDERMAN, "Statistical Theory of Fission Chains and Generalized Poisson Neutron Counting Distributions," *Nucl. Sci. Eng.* **172**, 300-326 (2012). 5, 6, 12

[8] K. BÖHNEL, "The effect of Multiplication on the Quantitative Determination of Spontaneously Fissioning Isotopes by Neutron Correlation Analysis," *Nucl. Sci. Eng.*, **90**, 75 (1985). 5, 10, 12

[9] M. PRASAD, N. SNYDERMAN, J. VERBEKE, R. WURTZ, "Time Interval Distributions and the Rossi Correlation Function," *Nucl. Sci. Eng.* **174**, 1-29 (2013). 10, 11

[10] K.S. KIM, L. NAKAE, M.K. PRASAD, N.J. SNYDERMAN, J.M. VERBEKE, "Time evolving fission chain theory and fast neutron and γ-ray counting distributions," LLNL-JRNL-658859-DRAFT , Lawrence Livermore National Laboratory, submitted to *Nucl. Sci. Eng.* (2015). 10